

Article

Sustainable Improvement of the Crack Resistance of Cohesive Soils

Michael Z. Izzo¹ and Marta Miletic^{2,*} 

¹ Department of Civil Engineering, Auburn University, Auburn, AL 36849, USA; mzi0006@auburn.edu

² Department of Civil, Construction, and Environmental Engineering, San Diego State University, 5500 Campanile Dr, San Diego, CA 92182, USA

* Correspondence: mmiletic@sdsu.edu

Received: 6 September 2019; Accepted: 16 October 2019; Published: 19 October 2019



Abstract: Desiccation cracking of cohesive soils is the development of cracks on the soil surface as a result of a reduction in the soil moisture content. The decrease in soil surface area owing to the desiccation of cohesive soils has an undesirable impact on the mechanical, hydrological, thermal, and physico-chemical properties. Many efforts have been made to improve the desiccation crack resistance of cohesive soils, but the current solutions raise a number of environmental issues, increasing the demand for sustainable soil improvement alternatives. Therefore, the main objective of this study is to investigate novel eco-friendly soil improvement techniques, such as recycled carpet fibers and a gelatin-based bioplastic, and their effect on desiccation cracking in cohesive soils. The improvement of soil crack resistance was studied by conducting desiccation cracking tests on plain and improved soils. In addition, image processing was conducted to quantitatively describe the effect of soil improvement type on the geometrical characteristics of crack patterns. Each soil improvement technique enhanced the soil strength and reduced cracking at room temperature, at an elevated temperature, and when subjecting to cyclic wetting and drying. The addition of bioplastics proved to be the most effective solution, thus demonstrating a viable option to advance future sustainable engineering practices.

Keywords: sustainable materials; ground improvement; image analysis; desiccation cracking

1. Introduction

Desiccation cracking is the development of cracks at the soil surface and throughout the depth of a cohesive soil layer as a result of soil shrinkage due to the reduction of the water content through solar radiation or vegetation absorption. The desiccation of cohesive soils leads to an undesirable impact on the mechanical, hydrological, thermal, and physico-chemical soil properties. For instance, desiccation cracking can lead to decreased soil strength which in turn can cause uneven settlement and catastrophic failures in structures of all types. In addition, this type of soil cracking results in a dramatic increase in the permeability of clayey soils. The increase in soil permeability is particularly problematic when the clay is used as a liner for both landfills and hazardous waste storage [1]. Therefore, the prevention of desiccation cracking is of significant importance to safety, structural, and environmental issues.

Due to the lack of an accepted American Society for Testing and Materials (ASTM) standard, desiccation tests have been conducted in a variety of ways with different boundary conditions, specimen geometry, and properties measured [1–5]. By utilizing a bar of clay seated on a grooved plate, the cracks only propagate in that same direction, creating a series of parallel cracks that can be easily analyzed for aperture and spacing [3]. More realistic two-dimensional (2D) cracking patterns can be obtained as a result of a complete horizontal constraint, allowing for crack intersections to be studied [1]. Therefore, it can be deduced that the geometry of the crack pattern depends strongly on the nature of the boundary

conditions and the sample geometry [3]. A parameter called the crack distribution frequency has been developed to evaluate the change in the area of a sample relative to a sample's original surface area [5]. A similar measurement, the crack intensity factor, has also been developed to analyze the ratio of the area of the cracks to the total specimen area [2]. In addition to the surface crack analysis, the crack depth can be analyzed using either manual means or more advanced image analysis techniques.

Image analysis has proven to be an incredible tool to quantitatively analyze crack characteristics in natural and humanmade geomaterials. To this end, several experimental test methods have been suggested and developed to assess the desiccation crack initiation and propagation within the different geomaterials. These include an analysis of images acquired with a scanning electron microscope (SEM) [6,7], a 2D profile laser [4,8] and different digital image acquisition systems [1,2,5]. A SEM has been extensively used to analyze micro-cracking in concrete and rocks [6] and to evaluate the effect of sodium chloride on the cracking of bentonite clay samples [7]. Despite the power of this technique, the main SEM drawback is its destructive nature. In particular, the specimen needs to be cut into thin slices and the sample faces need to be polished to make cracks and material constituents visible before taking high-resolution 2D images. Furthermore, due to the destructive and complex specimen preparation, the gradual propagation of a single crack cannot be studied. The 2D laser profile imaging has been successfully utilized in studying the propagation and geometry of desiccation cracking in clay soils [4] and the soil curling as a result of soil dehydration [8]. While 2D profile lasers are powerful tools to study desiccation cracking, their initial high price creates a barrier to entry for the academic and industry communities. All of these shortcomings are resolved by utilizing a user-friendly inexpensive digital image acquisition system to analyze the cracking behavior of clay soils.

To resolve safety, structural, and environmental issues caused by desiccation cracking, chemical additives, such as cement and lime, are used as binding agents to increase a clay's strength and resistance to cracking [9]. However, the current solutions have negative implications on the environment such as CO₂ emissions, the prevention of the vegetation growth, and the contamination of groundwater among others [7]. To rectify this, several research studies have been conducted in order to determine the viability of different sustainable soil-strengthening additives. The soil additives are considered sustainable if they have originated and have been refined from the industrial waste which remains toxic and hazardous to the environment when left unattended [10]. While this repurposing does not eliminate all negative side effects of the material as a waste product, it does prevent the negative effects of the use of alternative solutions [10]. The most commonly used sustainable soil additives are fly ash from thermal power plants [10–12], furnace slag from the steel industry [13,14], silica fume from the silicon and ferrosilicon industry [2,7,15,16], and carpet waste [17–19].

Chloride salts, such as ammonium chloride (NH₄Cl) and ferric chloride (FeCl₃), have demonstrated the ability to stabilize the volume of clays with high swelling potential [15]. The cations in the compounds reduce the swelling of montmorillonite minerals by replacing the interlayer metallic cations [16]. Furthermore, bentonite samples treated with sodium chloride (NaCl) developed cracks with greater lengths, but the overall crack density was significantly lower [7]. This was due to the effect of salt on the bentonite colloidal interactions that alter the double layer and particle association in a clay slurry [7]. Kalkan [15] used silica fume waste material as a sustainable alternative, and it was shown to significantly reduce desiccation cracking in clay liner systems.

The different types of fibers have also been examined as potential solutions to desiccation cracking [2,7,20]. Recycled carpet fibers have been lightly investigated as a potential soil improvement technique, with most studies being focused on the improvement of the strength properties of granular soil [18,19]. More recently, they have been examined as a potential method to reduce the swelling properties of cohesive soils [17]. The recycled carpet fibers were shown to decrease swelling pressure, with a 1% fiber content providing the most significant pressure drop [17]. Other unsustainable, fiber reinforcements have been shown to cause a significant reduction of desiccation cracking in expanding clay, with crack width decreasing by 50% [20]. Polypropylene fiber reinforcement has been proven to prevent tension crack growth in soils and stabilize soils against shrinking by increasing the soil's tensile

strength [7]. In addition, polypropylene fibers have been utilized to reinforce clay liners, leading the liners to be more rigid in compression and more ductile in tension [11]. The soils treated with fibers have also been shown to perform better than unreinforced soils when exposed to wetting and drying cycles [20].

Other forms of industrial waste have been examined as potential soil improvement techniques [11,12,21,22]. Fly ash has shown the ability to reduce plastic strain in clay soils when exposed to freeze-thaw cycles [12]. In addition, fly ash has been shown to increase compressive strength and produce similar behavioral trends to Portland cement [11]. The use of limestone waste has been shown to reduce the swelling properties of soil, producing a more compact microstructure when examined using SEM imaging [21]. Milled brick debris has also been shown to improve the compressive strength of soils when tested using the unconfined compression test [22].

This study seeks to investigate novel eco-friendly soil improvement techniques and their effect on the desiccation cracking behavior of soils. Three sustainable soil improvement techniques were tested, including fly ash, recycled carpet fibers, and bioplastic. Both recycled carpet fibers and fly ash were considered sustainable materials under the idea that repurposed industrial waste is a sustainable material. Numerous studies have been conducted investigating the effects eco-friendly additives have on soil strength and swelling properties, yet their effect on the crack resistance of cohesive soils has been largely under-investigated. To date, neither recycled carpet fibers nor bioplastics have been examined as a potential solution to desiccation cracking and their effectiveness is presented in this research. This is also the first study to compare these techniques at two different temperatures and to subject them to cyclic wetting and drying. Consequently, a comparative analysis of the mentioned improvement techniques' effectiveness has not been completed. A qualitative analysis was conducted by analyzing the geometric characteristics of cracking patterns in the plain and improved soil samples. The quantitative analysis was completed using an original code powered by MATLAB's image analysis software before performing image matrix operations in a Visual Basic for Applications (VBA) program. The utilized image analysis process is simple and inexpensive due to the widespread public familiarity and access of both VBA and MATLAB. A comparative analysis of the soil improvement techniques was completed using the area reduction factor (ARF), average crack width (w_{avg}) and maximum crack width (w_{max}) of the treated and non-treated cohesive soil samples.

2. Materials and Methods

2.1. Materials

2.1.1. Base Soil

The base soil material used for experimentation was residual Piedmont soil that had been sieved through the No. 40 sieve (0.425 mm). Piedmont soils have the reputation of not being particularly well categorized by the Unified Soil Classification System (USCS) [23]. The soil behaves almost as a hybrid soil type, exhibiting characteristics of the fine-grained silt in undrained conditions and the coarse-grained soil silty sand in drained conditions when loading is applied [23]. Figure 1 depicts the grain size distribution curve for the base soil. The soil was tested for its Atterberg Limits in accordance with ASTM D4318 [24] and the liquid limit and plasticity Index were determined to be 49 and 20, respectively. Therefore, according to the USCS, the fine particles are classified as silt with low plasticity. The overall classification of residual Piedmont soil that was used in this study was well-graded sand with silt (SW-SM).

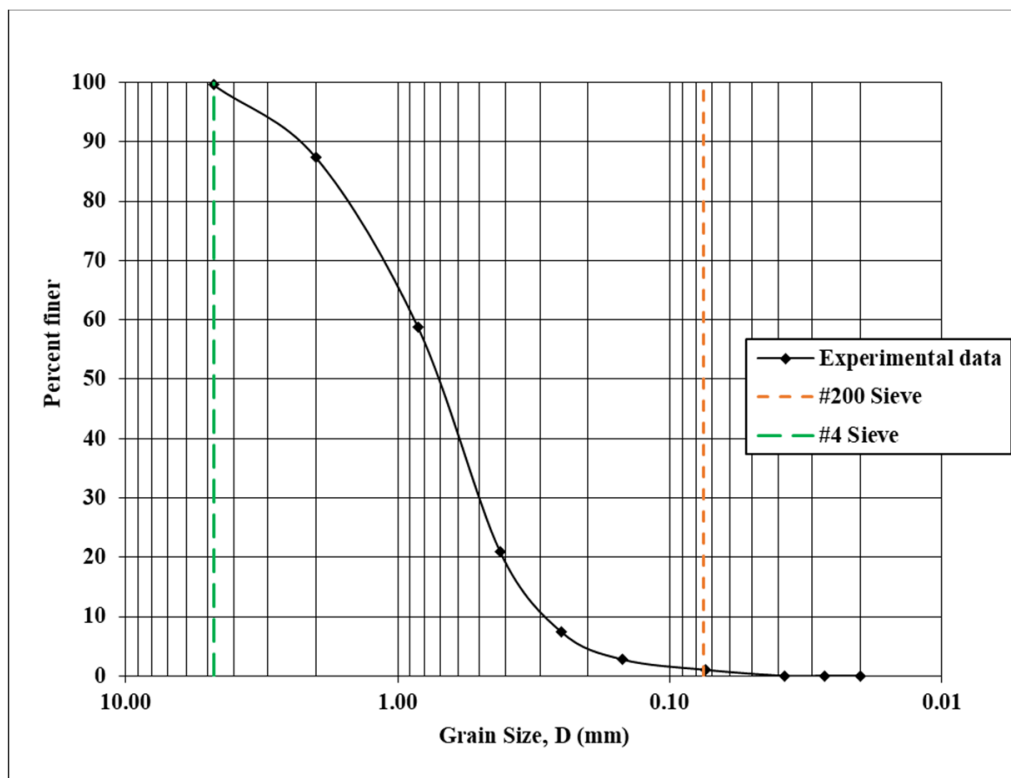


Figure 1. Grain size distribution curve of the base soil used in this study.

2.1.2. Soil Improvement Types

In this study, the three additives investigated as strengthening agents were fly ash, recycled polyester carpet fibers, and bioplastic, as well as a fly ash-fiber combination. The first tested improvement technique was Class C fly ash. This is the light weight waste produced by burning pulverized coal. It has cementitious qualities and is often used as an additive during the concrete mixing procedure. The fly ash addition was 15% based on the dry weight of the soil.

The next soil improvement technique was introducing recycled polyester carpet fibers to the soil samples. The polyester fibers were short straight fibers manufactured by Beaulieu of America, USA, and had a length of 50 mm and a diameter of 0.07 mm (aspect ratio of 714). The density of the polyester fibers was 1.38 g/cm^3 (20°C), and the volumetric fiber content was one per cent.

A combination of the Class C fly ash and the carpet fibers was also tested as an improvement technique. The base material and fly ash were mixed first, where the fly ash addition was 10% based on the dry weight of the soil. After the initial dry mixture was complete, polyester fiber was added until the sample contained 0.5% fibers by volume. All the addition rates of fly ash and carpet fibers were determined by a critical and extensive review of the existing literature, and preliminary laboratory mix design testing.

The final soil improvement technique analyzed was a gelatin-based bioplastic. The gelatin-based bioplastic concentration was 8%. To achieve this, for every 500 g of base material used, 44 g of water, 30 g of vinegar, 7.2 g of gelatin, and three grams of glycerin were mixed together. To prepare the gelatin-based bioplastic, the water was boiled on a hot plate, with the gelatin being slowly added to prevent clumping. The vinegar and glycerin were then subsequently slowly mixed into the final blend. After thoroughly mixing all of the components, bioplastic was added to the base material sample soil and mixed again, until the homogenous soil-bioplastic mixture was achieved.

2.2. Methods

2.2.1. Desiccation Test

The desiccation crack test was performed on improved and non-improved soil specimens. The purpose of the desiccation test was to study the cracking behavior of a soil sample as the sample reduces the moisture content and dehydrates. The samples were prepared by first mixing all the dry components (base soil, fly ash, fibers) together for a few minutes and then water was added to raise the water content to the desired level of 25%. The bioplastic-treated sample was prepared in the manner described in the materials section. Once thoroughly mixed, the soil specimens were manually placed into the cylindrically-shaped, lubricated stainless-steel molds and lightly smoothed to have a uniform clay thickness of 20 mm. The inner diameter of the mold was 230 mm.

In order to study the temperature effect on the desiccation crack cracking and soil-improvement type, two different types of desiccation tests were performed: standard and accelerated. During the standard test, the sample was allowed to dry at constant room temperature (20 °C) and humidity (80%) for 24 straight hours. Each soil sample was tested under the same conditions. The samples were consistently monitored for the first eight hours and then a final check was performed at the 24-h mark. For the accelerated test, the samples were heated in the oven at 105°C for two hours before rewetting the sample and completing the process for another two hours. Every fifteen minutes, the soil sample was carefully removed for image acquisition and then immediately replaced in the oven. After two hours, water was slowly poured over the sample until the initial water content was reached. The sample was then placed into the oven and allowed to dry for another two hours, with continued monitoring and image acquisition every 15 min.

2.2.2. Image Acquisition and Processing

The digital images of the soil samples were taken at fixed time increments using a stand held at a constant position for image consistency and uniformity. The camera was placed on a stand 46 cm tall that was fixed over the center of the clay sample. The image acquisition time frame increments were 15 and 120 min for the standard test and accelerated tests, respectively. For each image, the number of cracks in the specimen with a length of at least one centimeter was counted and recorded.

The digital image acquisition was followed by image processing to identify each constitutive component (cracks, fibers, and soil matrix) and, finally, a quantitative analysis of the crack geometric properties within the sample. In order to do so, the original MATLAB code was developed in this study. The image processing program consisted of six major steps to achieve the desired crack parameters.

The first step, image conversion, converted the original digital image (Figure 2a) first into a grayscale image and then further still into a binary image (Figure 2b). The second step was segmentation which isolated the clay surface and removed blemishes from the indentations in the clay surface (Figure 2c). The image was then given real dimensions by converting a known distance in the image to a pixel distance, giving the image data context. The surface area of each specimen was collected and the initial area ($Area_i$) for each specimen was stored and compared to each subsequent image. The change in the area at each stage ($\Delta Area$) in comparison with the initial area ($Area_i$) was used to determine the ARF:

$$ARF = \frac{\Delta Area}{Area_i} \quad (1)$$

To accurately analyze the crack parameters, the binary image of the crack needed to be isolated such that the desiccation crack was the only black portion of the image remaining (Figure 2d). This final image was analyzed using a VBA code to return values for the maximum crack width (w_{max}) and the average crack width (w_{avg}).

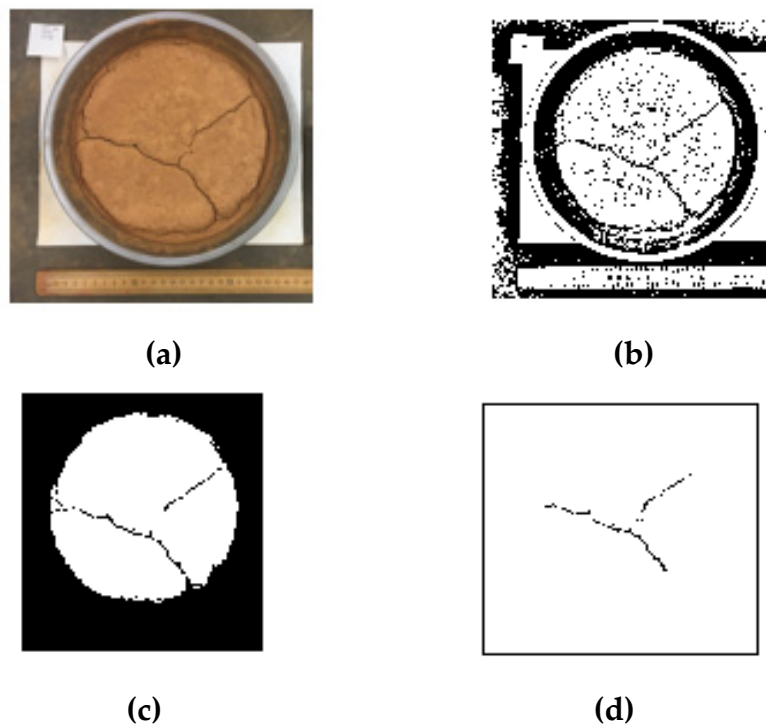


Figure 2. Image processing: (a) original sample photo; (b) original binary image; (c) clay surface binary image; (d) isolated crack binary image.

3. Results

Using the data obtained from the image analysis, the performance of each soil improvement technique was examined. The final crack count, w_{avg} , and w_{max} were recorded at each time frame during the accelerated desiccation test. In general, the cracks developed rapidly, with the samples often going from no cracks to a fully-realized crack network in one photocycle (15 min time frame). The development of the desiccation cracking throughout the first drying cycle of the accelerated test can be seen in Figure 3. The figure shows that the cracking pattern of the base soil sample propagated in a three-pronged, letter Y-like shape (Figures 3 and 4). However, the specimens with the ash and fibers sometimes deviated from this shape. Once the samples with the added fiber cracked in the second cycle, they took on a more circular manner like the letter C with smaller segments radiating out to the edges (Figure 5). This was most likely due to the transverse isotropic fiber distribution as a result of the clay mixing process. As the clay was mixed in a circular motion, many of the fibers became orientated in the same pattern. Consequentially, the cracks formed parallel to the fiber alignment because of the lack of reinforcement oriented perpendicular to the crack. The fly ash samples tended to have a more lopsided shape and propagated in a more clustered manner.

For the standard desiccation test, only the *ARF* results were recorded for each chronologic digital image due to crack propagation not occurring at room temperatures during the first eight hours of the testing process. The final crack count, w_{avg} , and w_{max} were recorded at the 24-hour mark.

The crack count was recorded in order to quantitatively analyze the crack network morphology. The results from the standard desiccation test can be seen in Figure 6. The figure shows that aside from adding the gelatin-based bioplastic, the soil additives did not materially affect the total number of crack segments after 24 h of drying at room temperature. Both samples that included fly ash developed an additional crack segment over the untreated soil.

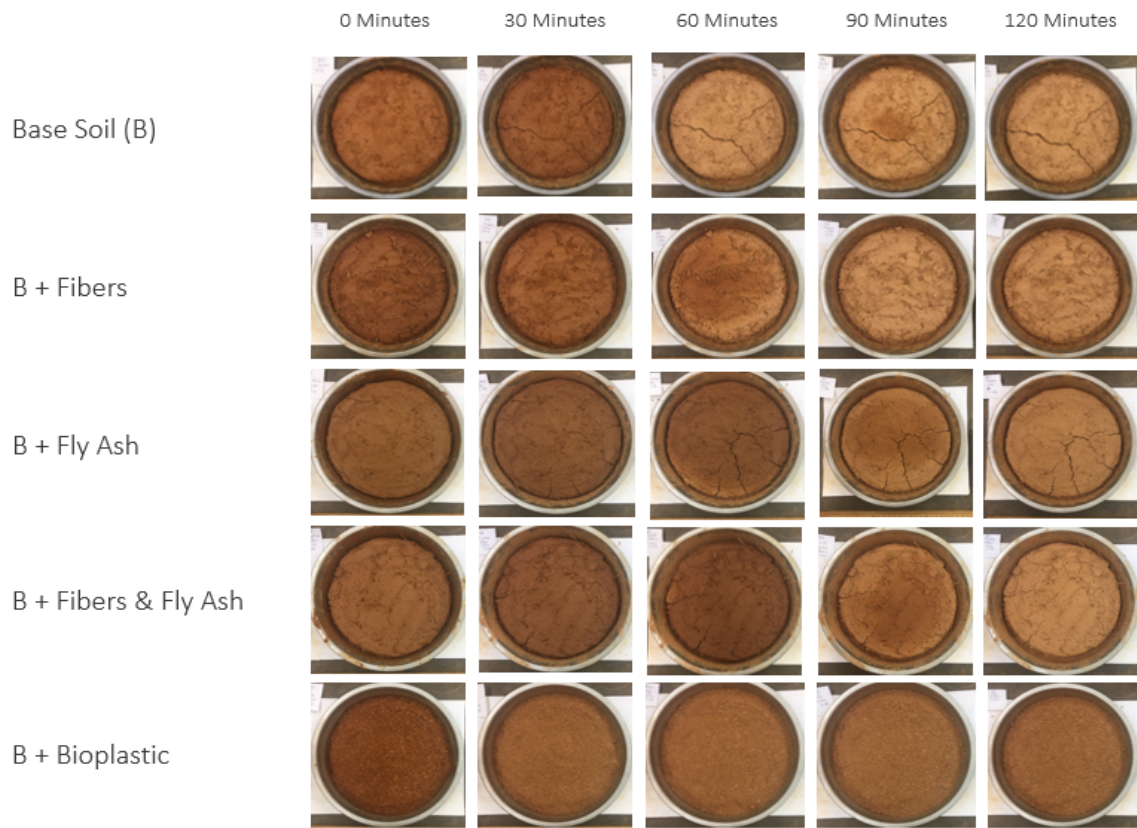


Figure 3. Desiccation crack test results for accelerated test after two hours of drying.



Figure 4. Desiccation crack test results for accelerated test for base soil.



Figure 5. Accelerated test final crack distribution for fiber-aided soil.

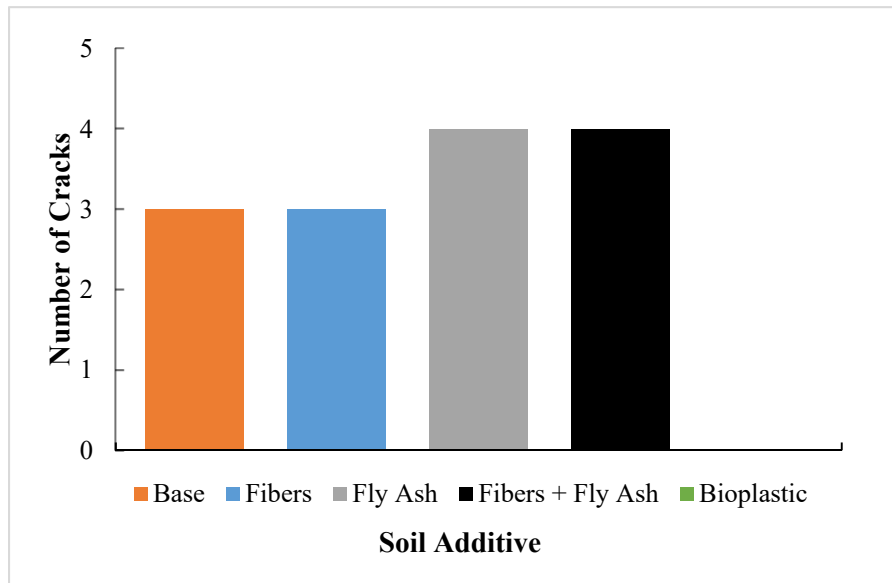


Figure 6. Number of cracks developed in standard desiccation test after 24 h at room temperature.

The crack count data for the accelerated desiccation test can be seen in Figure 7. The figure shows that in the first drying cycle (Figure 7a), no cracks developed in the samples mixed with the bioplastic and with the carpet fibers only. In the samples where cracks did develop, they generally appeared between the 15- and 30-min marks. After the rewetting process (Figure 7b), the bioplastic-improved soil sample was the only sample that did not develop any desiccation cracks. Each of the other additives developed more cracks than the base soil at the end of the second drying cycle. After rewetting, the timing of crack formation varied to a much greater degree with the plain soil cracking after 15 min, the fiber-aided soil cracking after 30 min, the fly ash sample developing cracks at the 45-minute mark, and the hybrid additive preventing cracking up until 75 min after rewetting occurred.

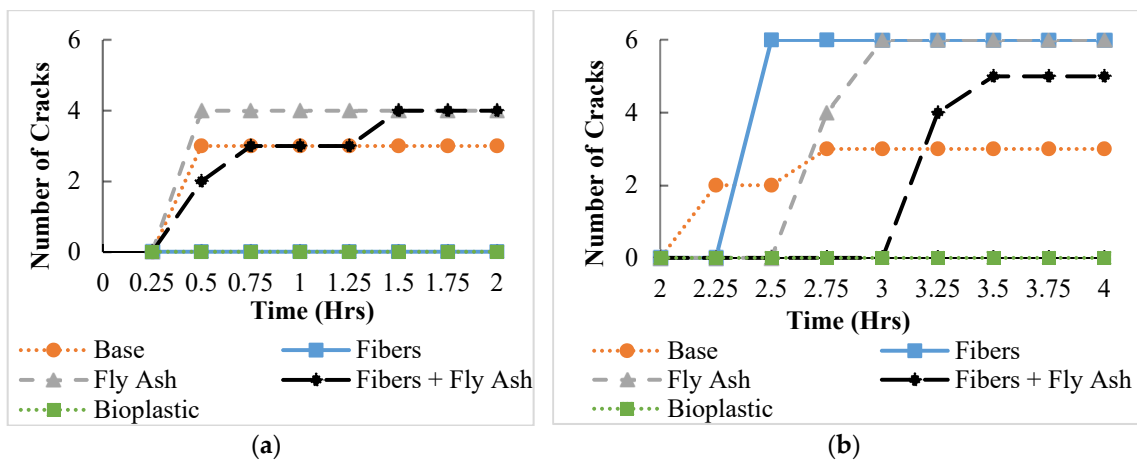


Figure 7. Development of the desiccation cracks in the accelerated test: (a) first drying cycle; (b) second drying cycle.

The w_{avg} was calculated so that each soil improvement method’s ability in solely reducing crack growth could be examined. The effect of the different soil improvement type on the w_{avg} for the standard desiccation test can be seen in Figure 8. The average crack width after 24 h for the base soil was found to be 1.59 mm. The sample with fly ash showed almost no improvement over the plain specimen. The samples improved with only carpet fibers and the carpet fibers-fly ash combination developed

cracks with smaller average widths of approximately 0.9 mm at the end of testing. The sample with the bioplastic had no average crack width as it did not develop cracks during the standard desiccation test.

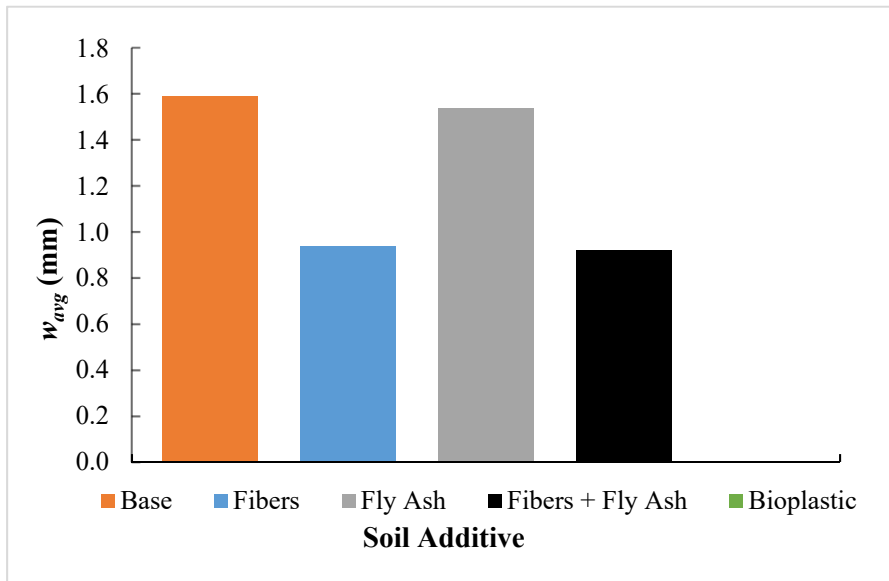


Figure 8. Average crack width of soils under standard desiccation test at 24-hour mark.

The effect of different soil improvement types on the w_{avg} for the accelerated desiccation test is depicted in Figure 9. The average crack width at the end of the wetting and drying process for the base soil was found to be 1.54 mm (Figure 9b). The samples with fly ash and carpet fibers showed almost no improvement in comparison with the non-treated soil. The samples with carpet fibers-fly ash combination developed cracks with smaller average widths at the termination point. The sample with the bioplastic did not develop cracks during the test and therefore had no average crack width. It is worth noting that the crack width after rewetting was assumed to be zero. Though some soil damage can be observed, the full depth cracks were not present at the time. In addition, in some time periods, the average crack width was shown to decrease. This was not due to the cracks shrinking, but as a result of the image processing software reading darker, wet spots in the soil near the cracks as parts of the actual crack. As the soil dried out more, the wet spots disappeared, causing the cracks to appear to be narrowing.

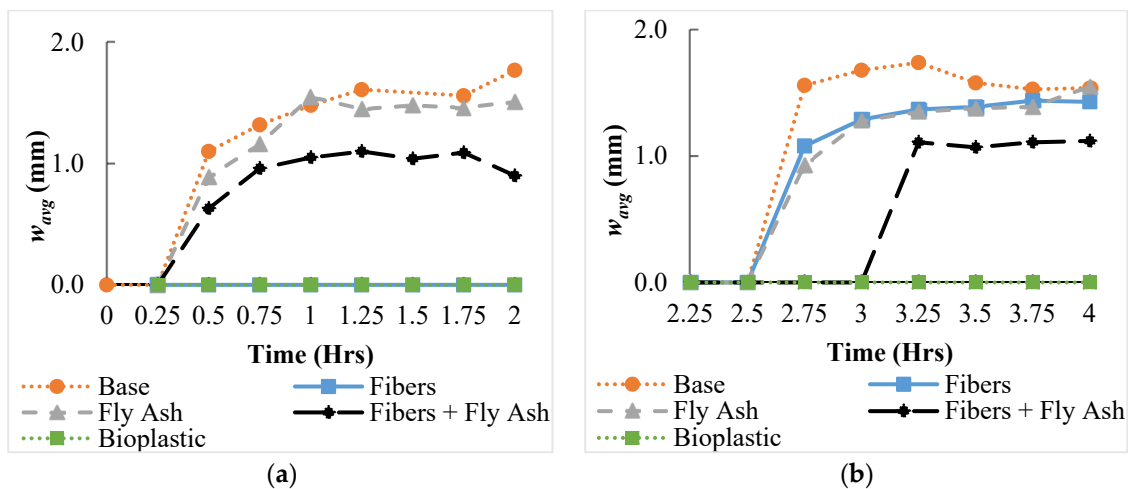


Figure 9. The effect of the soil improvement type on the development of the average crack width, w_{avg} in the accelerated test: (a) first drying cycle; (b) second drying cycle.

The effect of the different soil improvement types on the maximum crack width, w_{max} for the standard desiccation test can be seen in Figure 10. The reasons for finding the maximum crack width in each sample were twofold. First, the wider cracks have a greater potential to cause structural damage, meaning the maximum crack width represents the greatest potential for failure. Second, it provides context for the average crack results. For example, the fly ash sample possessed a w_{avg} similar to that of the untreated soil, however, the w_{max} of the fly ash was approximately 2 mm greater than the base soil. This suggests that the fly ash most likely had a segment with an abnormally large crack with the remainder of the cracks being narrower than the cracks in the base soil. The maximum crack width at the end of the test for the base soil was found to be 4.11 mm. The sample with fly ash developed a crack system with a wider maximum crack width than the base clay (6.32 mm). The samples with just carpet fibers and the carpet fibers plus fly ash developed cracks with significantly smaller maximum widths of approximately 2.08 mm and 2.38 mm, respectively, at the end of testing. Again, the sample treated with the gelatin-based bioplastic never cracked during the desiccation test.

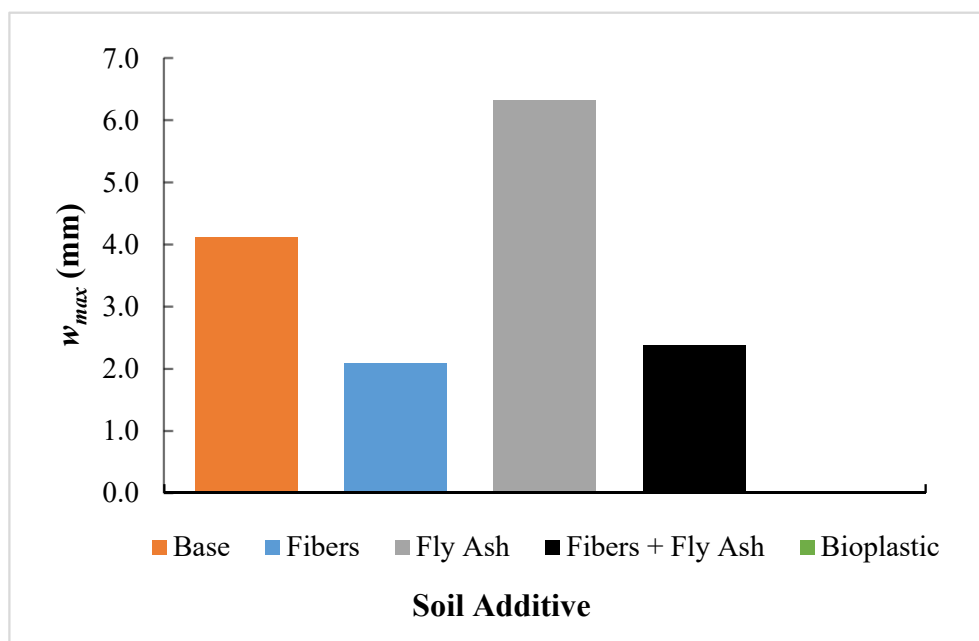


Figure 10. The effect of different soil improvement types on the maximum crack width, w_{max} at the 24-h mark.

The maximum crack widths over both drying cycles for each soil improvement type are shown in Figure 11. Each of the additives reduced the maximum crack width at the end of the testing process in comparison to the base soil but to varying degrees. Again, the sample with the gelatin-based bioplastic exhibited no changes and no cracking occurred. The samples with each of the fly ash only and the recycled carpet fiber showed approximately the same level of maximum crack width reduction, while the sample with the combined additives provided further crack reduction. In the second cycle, the plain soil's maximum crack width exhibited the same soil drying phenomenon that affected the average crack width results and led to the appearance of crack narrowing.

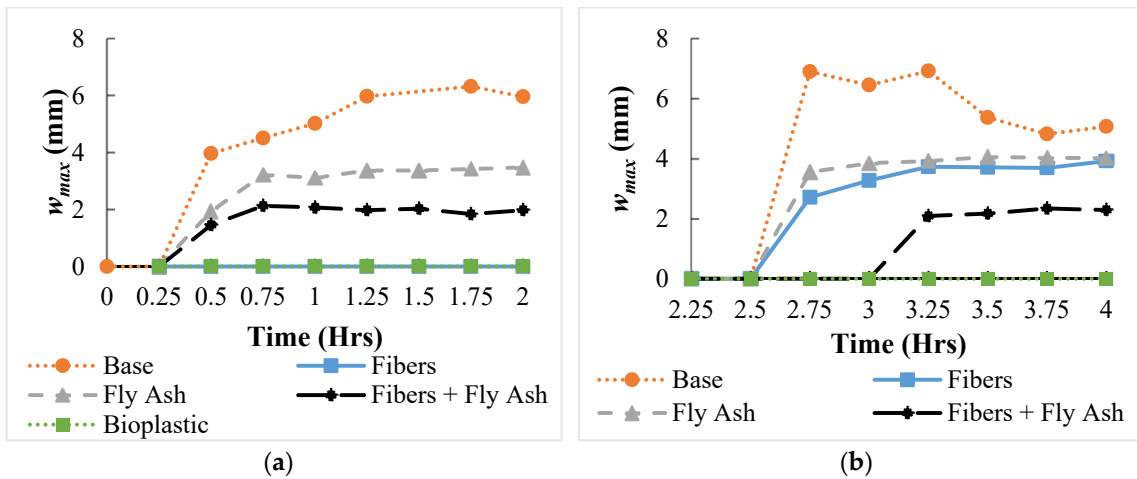


Figure 11. The effect of the soil improvement type on the development of the maximum crack width, w_{max} in the accelerated test: (a) first drying cycle; (b) second drying cycle.

The *ARF* parameter was introduced to quantitatively measure the effectiveness of each soil improvement technique in reducing desiccation cracking as well as the overall soil shrinkage. The efficacy of the respective additives for the standard desiccation test can be seen in Figure 12. The figure shows that the base material exhibits the greatest *ARF* and the bioplastic exhibits virtually no shrinkage and did not crack after 24 h. Even though no cracks developed in any specimens until the 24-h mark, the samples still had *ARF* values due to lateral shrinkage of the samples before cracking. By analyzing the images, it was determined that the variations in the short-term were caused by discoloration in the clay surface as a result of uneven drying.

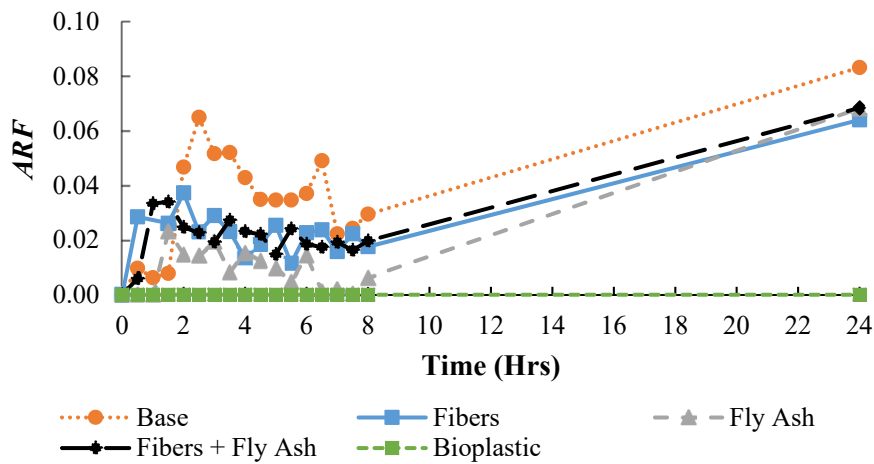


Figure 12. The effect of the different soil improvement type on the development of the *ARF* in the standard desiccation test.

For the accelerated desiccation test, the results from before and after the rewetting process were analyzed. The *ARF* data for both the initial drying cycle and the drying cycle after rewetting are displayed in Figure 13 a and b, respectively. The results showed that the samples including the fly ash provided little improvement when exposed to higher temperatures. Again, the sample mixed with the gelatin-based bioplastics showed no change in the surface area even when exposed to higher temperatures.

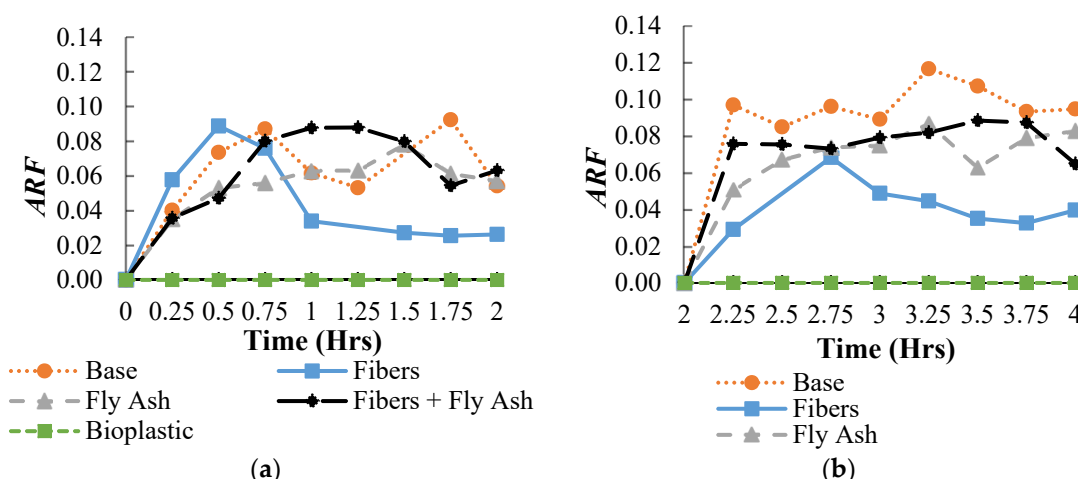


Figure 13. The effect of the soil improvement type on the *ARF* in the accelerated test: (a) first drying cycle; (b) second drying cycle.

4. Conclusions

The main aim of this research is the development of novel, eco-friendly soil improvement techniques and the investigation of their effect on the desiccation cracking behavior. In particular, three different sustainable soil improvement types were investigated, namely, fibers, bioplastics, and fly ash, along with a fly ash-fiber hybrid. The effect on the cohesive soils' crack resistance from the addition of a bioplastic and recycled carpet fibers were examined for the first time. In addition, the effectiveness of the techniques for crack resistance were examined at different temperatures and when subjected to cyclic wetting and drying for the first time.

A qualitative analysis was conducted by analyzing the geometric characteristics of the cracking patterns in the plain and sustainably improved soil samples. It was completed using an original code powered by MATLAB's image analysis software before performing image matrix operations in VBA program. MATLAB's image processing software proved to be a powerful tool in quantifying the 2D cracking behavior of the clay soils. By converting photos of the clay samples into representative matrices, each sample's crack geometry could be quickly and accurately attained. This is a vast improvement over the time consuming, expensive, and mostly inaccurate manual methods that have been employed to measure cracking behavior.

The *ARF* provided a comparative measurement that incorporated surface area change due to cracking as well as global shrinkage of the clay samples. The average crack width and maximum crack width data further described the crack geometry and each improvement techniques' effectiveness in reducing the scope of desiccation cracking. The bioplastic proved to be the most effective technique, completely preventing cracking and surface area reduction at room temperature, elevated temperatures and when subjected to a wetting and drying cycle. The fly ash treatment was able to reduce the width of the cracks when subjected to increased temperature but supplied little improvement over the untreated soil in terms of the total surface area reduction. Conversely, when dried slowly at room temperature, the same treatment technique yielded wider cracks than the base soil, but did show a 25% improvement in terms of *ARF*. The fiber-reinforced samples showed a sustained decrease in the crack size in each scenario, except for when the sample was being dried a second time after the rewetting process. At that point, the fiber-reinforced soil showed little improvement in minimizing the crack size, but still reduced *ARF* by 60%. The sample treated by the fiber-fly ash combination significantly decreased the size of cracks in all scenarios. However, this treatment showed little improvement over the base soil when subjected to a higher temperature with regards to the *ARF*. In addition, the combination fared worse than the soil treated solely by fibers. The behavior of the fly ash treated samples and the combined sample suggests that fly ash loses its effectiveness when subjected to higher temperatures.

The results included in this paper are part of a larger research project examining the viability of novel sustainable soil improvement techniques. Moving forward, more research into sustainable desiccation crack reduction is warranted. Based on the success in this investigation, other recycled fibers should be studied to determine their viability. Due to the bioplastic's overwhelming performance as a crack propagation reducer, biopolymers that behave similarly to the bioplastic, such as guar gum and xanthan gum, should be closely examined as potential solutions to desiccation cracking.

Author Contributions: Conceptualization, M.M. and M.Z.I.; methodology, M.Z.I.; software, M.Z.I.; validation, M.M. and M.Z.I., writing—original draft preparation, M.Z.I.; writing—review and editing, M.M.; supervision, M.M.

Funding: This research received no external funding.

Acknowledgments: The authors would like to thank the Highway Research Center at Auburn University and 100+ Women Strong-New Faculty Undergraduate Research Award for sponsoring this project.

Conflicts of Interest: The authors declare no conflicts of interest.

References

1. Laloui, L.; Peron, H.; Hueckel, T.; Hu, L.B. Desiccation Cracking of Soil. *Eur. J. Environ. Civ. Eng.* **2009**, *13*, 869–888.
2. Chaduvula, U.; Viswanadham, B.; Kodikara, J. A study on desiccation cracking behavior of polyester fiber-reinforced expansive clay. *Appl. Clay Sci.* **2017**, *142*, 163–172. [[CrossRef](#)]
3. Peron, H.; Hueckel, T.; Laloui, L.; Hu, L.B. Fundamentals of desiccation cracking of fine-grained soils: Experimental characterisation and mechanisms identification. *Can. Geotech. J.* **2009**, *46*, 1177–1201. [[CrossRef](#)]
4. Sánchez, M.; Atique, A.; Kim, S.; Romero, E.; Zielinski, M. Exploring desiccation cracks in soils using a 2D profile laser device. *Acta Geotech.* **2013**, *8*, 583–596. [[CrossRef](#)]
5. Suits, L.D.; Sheahan, T.C.; Lakshmikantha, M.R.; Prat, P.C.; Ledesma, A. Image Analysis for the Quantification of a Developing Crack Network on a Drying Soil. *Geotech. Test. J.* **2009**, *32*, 102216. [[CrossRef](#)]
6. Arena, A.; Piane, C.D.; Sarout, J. A new computational approach to cracks quantification from 2D image analysis: Application to micro-cracks description in rocks. *Comput. Geosci.* **2014**, *66*, 106–120. [[CrossRef](#)]
7. Shokri, N.; Zhou, P.; Keshmiri, A. Patterns of Desiccation Cracks in Saline Bentonite Layers. *Transp. Porous Media* **2015**, *110*, 333–344. [[CrossRef](#)]
8. Zielinski, M.; Sánchez, M.; Romero, E.; Atique, A. Precise observation of soil surface curling. *Geoderma* **2014**, *226*, 85–93. [[CrossRef](#)]
9. Shah, M.; Pandya, H.; Shukla, A. Influence of Chemical Additives on Shrinkage and Swelling Characteristics of Bentonite Clay. *Procedia Eng.* **2017**, *189*, 932–937. [[CrossRef](#)]
10. Jayanthi, P.N.V.; Singh, D.N. Utilization of Sustainable Materials for Soil Stabilization: State-of-the-Art. *Adv. Civ. Eng. Mater.* **2016**, *5*, 20150013. [[CrossRef](#)]
11. Consoli, N.C.; Marin, E.J.B.; Samaniego, R.A.Q.; Heineck, K.S.; Johann, A.D.R. Use of Sustainable Binders in Soil Stabilization. *J. Mater. Civ. Eng.* **2019**, *31*, 06018023. [[CrossRef](#)]
12. Wei, H.; Li, Q.; Han, L.; Han, S.; Wang, F.; Zhang, Y.; Chen, Z. Experimental Research on Deformation Characteristics of Using Silty Clay Modified Oil Shale Ash and Fly Ash as the Subgrade Material after Freeze-Thaw Cycles. *Sustainability* **2019**, *11*, 5141. [[CrossRef](#)]
13. Kamon, M.; Nontananandh, S. Combining Industrial Wastes with Lime for Soil Stabilization. *J. Geotech. Eng.* **1991**, *117*, 1–17. [[CrossRef](#)]
14. Wild, S.; Kinuthia, J.M.; Robinson, R.B.; Humphreys, I. Effects of ground granulated blast furnace slag (GGBS) on the strength and swelling properties of lime-stabilized kaolinite in the presence of sulphates. *Clay Miner.* **1996**, *31*, 423–433. [[CrossRef](#)]
15. Kalkan, E. Influence of silica fume on the desiccation cracks of compacted clayey soils. *Appl. Clay Sci.* **2009**, *43*, 296–302. [[CrossRef](#)]
16. Zumrawi, M.M.E.; Mahjoub, A.M.M.; Alnour, I.M. Effect of Some Chloride Salts on Swelling Properties of Expansive Soil. *Univ. Khartoum Eng. J.* **2016**, *6*, 35–41.
17. Mirzababaei, M.; Miraftab, M.; Mohamed, M.; McMahan, P. Impact of Carpet Waste Fibre Addition on Swelling Properties of Compacted Clays. *Geotech. Geol. Eng.* **2012**, *31*, 173–182. [[CrossRef](#)]

18. Ghiassian, H.; Poorebrahim, G.; Gray, D.H. Soil reinforcement with recycled carpet wastes. *Waste Manag. Res.* **2004**, *22*, 108–114. [[CrossRef](#)]
19. Shahnazari, H.; Ghiassian, H.; Noorzad, A.; Shafiee, A.; Tabarsa, A.R.; Jamshidi, R. Shear modulus of silty sand reinforced by carpet waste strips. *J. Seismol. Earthq. Eng.* **2009**, *11*, 133–142.
20. Chaduvula, U.; Manogaran, I.; Viswanadham, B.V.S.; Kodikara, J. Some Studies on Desiccation Cracking of Fiber-Reinforced Expansive Clay Subjected to Drying and Wetting Cycles. *PanAm Unsaturated Soils 2017 2018*, *GSP 303*, 361–370.
21. Pastor, J.L.; Tomás, R.; Cano, M.; Riquelme, A.; Gutiérrez, E. Evaluation of the Improvement Effect of Limestone Powder Waste in the Stabilization of Swelling Clayey Soil. *Sustainability* **2019**, *11*, 679. [[CrossRef](#)]
22. Hidalgo, C.; Carvajal, G.; Muñoz, F. Laboratory Evaluation of Finely Milled Brick Debris as a Soil Stabilizer. *Sustainability* **2019**, *11*, 967. [[CrossRef](#)]
23. Mayne, P.W.; Brown, D.; Vinson, J.; Schneider, J.A.; Finke, K.A. Site Characterization of Piedmont Residual Soils at the NGES, Opelika, Alabama. *Natl. Geotech. Exp. Sites* **2000**, *GSP 93*, 160–185.
24. *ASTM D4318-00 Standard Test Methods for Liquid Limit, Plastic Limit, and Plasticity Index of Soils*; Annual Book of ASTM Standards, ASTM International: West Conshohocken, PA, USA, 2003; pp. 482–593.



© 2019 by the authors. Licensee MDPI, Basel, Switzerland. This article is an open access article distributed under the terms and conditions of the Creative Commons Attribution (CC BY) license (<http://creativecommons.org/licenses/by/4.0/>).